Transformations of magnetic mineralogy in rocks revealed by difference of hysteresis loops measured after stepwise heating: theory and case studies

Bernard Henry, Diana Jordanova, Neli Jordanova, Maxime Le Goff

HAL Id: insu-03601116

https://insu.hal.science/insu-03601116

Submitted on 8 Mar 2022

GJI Geomagnetism, rock magnetism and palaeomagnetism

Transformations of magnetic mineralogy in rocks revealed by difference of hysteresis loops measured after stepwise heating: theory and case studies

Bernard Henry,[1] Diana Jordanova,[2] Neli Jordanova[2] and Maxime Le Goff[1]

[1] *Géomagnétisme et Paléomagnétisme, IPGP and CNRS,* 4 *avenue de Neptune,* 94107 *Saint-Maur cedex, France. E-mail: henry@ipgp.jussieu.fr*
[2] *Geophysical Institute, Bulgarian Academy of Sciences, Acad. G. Bonchev Street, Block* 3, 1113 *Sofia, Bulgaria*

SUMMARY

A new approach for tracking mineralogical alterations during laboratory stepwise heating experiments is proposed. It uses the hysteresis loop obtained as a difference between the loops measured after thermal treatment at two different consecutive temperatures. Depending on the nature of the mineralogical alterations (the formation of a new ferrimagnetic phase from a paramagnetic one, the thermal transformation of the originally present ferrimagnetic phases, grain size variation) and on their relative intensities, it is possible to distinguish between different cases. The examples shown reveal the significant alteration of magnetic carriers at low temperatures (up to 200°C) which usually is not identified by thermomagnetic analysis of magnetic susceptibility. The low temperature alteration of the remanence carriers has important consequences for the reliability and suitability criteria of palaeointensity determinations.

Key words: hysteresis loop, mineralogical alteration, thermal treatment.

1 INTRODUCTION

Mineralogical alterations frequently occur in rocks subjected to thermal treatment. In many cases, laboratory heating may cause not only phase transformations, but also changes in the effective magnetic grain sizes, internal stress and oxidation state. These factors are crucial for the validity and success of the palaeointensity determinations, and the proper use of thermal enhancement in magnetic anisotropy studies, etc.

The least time-consuming and most common approaches to the study of such alterations during heating monitor the variations of bulk magnetic susceptibility measured at room temperature after successive thermal steps. This method, however, does not give reliable information about the real processes, insofar as the measured values reflect only the result of all the simultaneous changes in a complex mineralogical system such as natural rock. The aim of this work is to offer a complementary method resulting in better knowledge of the various alterations occurring during stepwise laboratory heating.

2 MINERALOGICAL ALTERATION STUDIES

Alterations of magnetic minerals can correspond to the formation of new ferrimagnetic minerals from paramagnetic phases, to the transformation of ferrimagnetic phases into other ferrimagnetic minerals, or to grain-size and various structural changes of ferrimagnetic carriers. Often, several of these mechanisms act at the same time,

but it is difficult to distinguish between them. Detailed studies are carried out on mineral characterization, magnetic properties and the thermomagnetic behaviour of thermally unstable magnetic rock-forming minerals such as iron sulphides (pyrite, pyrrhotite, greigite, troilite), carbonates (siderite, ankerite), silicates and iron oxides or hydroxides (e.g. Verwey 1935; Schwartz & Vaughan 1972; Gehring & Heller 1989; Dekkers 1990a,b; Özdemir 1990; Bina *et al.* 1991; Hirt & Gehring 1991; Henry *et al.* 2003, and references therein).

The most widely used method to monitor the alterations is based on measurements of the low-field magnetic susceptibility at room temperature after each heating step, for example during thermal demagnetization of natural remanent magnetization (NRM) or of saturation isothermal remanent magnetization (SIRM). Any change of susceptibility value indicates the occurrence of mineralogical alteration. No significant variation of the remanent magnetization but a strong susceptibility change after a thermal treatment indicates that the remanence carrier is not affected by the alteration. On the other hand, however, variation of both factors after the same treatment does not always imply alteration of the remanence carrier (the applied temperature could correspond to a blocking temperature). Van Velzen & Zijderveld (1992) proposed an alternative method for monitoring mineralogical alteration using several magnetic characteristics, which allows a much more precise study of the effect of heating. However, if several different alterations occur during the same thermal treatment, they still cannot be distinguished.

Recently, a study of the effect of progressive heating on magnetic fabric data was carried out based on an analysis of the difference of magnetic susceptibility tensors measured before and after

successive heating steps (Henry *et al.* 2003). Again, the obtained results concern the bulk mineralogical alteration, but the observed permutation of susceptibility axes in certain cases clearly shows that grain-size variations between single-domain (SD) and another grain size occurred.

We propose here a method based on the comparison of hysteresis loops measured at room temperature after successive heating steps. In fact, significant evolution of the shape of such loops arises when the ferrimagnetic part of the rock is affected by mineralogical alteration due to thermal treatment.

3 MODELLING THE DIFFERENCE HYSTERESIS LOOPS

A hysteresis loop (Fig. 1a) comprises two parts. In the 'descending' part 'd' (in this case d400 and d550), the magnetization J is measured during progressive field variation from high field applied in a chosen direction to high field in the opposite direction. The 'ascending' part 'a' (a400 and a550 in the example) is determined during progressive field variation from high field in this last direction to high field in the initial direction. During stepwise thermal demagnetization, a hysteresis loop is measured at room temperature T0 after each heating steep. The difference hysteresis loops ($J_{Tj} - J_{Ti}$), presented in Fig. 1(b), are obtained by subtraction of the two intensities (J_{Tj} and J_{Ti}) measured at a given applied field value (H), for two successive temperatures Tj and Ti respectively, with Tj > Ti (Ti ≥ T0): J_{Ti} measured in part 'd' of the loop is subtracted from J_{Tj} in the same part 'd' of the loop, and J_{Ti} obtained in part 'a' of the loop is subtracted from J_{Tj} in the corresponding part 'a' (Fig. 1b):

$$J_{Tj\,-Ti}\,(H) = J_{Tj}(H) - J_{Ti}(H). \tag{1}$$

Looking at the difference hysteresis loops obtained in this way, the disappearance of the ferrimagnetic phase corresponds to negative magnetization values, and the occurrence of a new phase to positive values. In the simple case of the appearance of a ferrimagnetic phase, the shape of the difference hysteresis loop is similar to that of a classical loop for this phase. For the case of the disappearance of a magnetic phase, the difference curve is a mirror-image relative to the *x*-axis of the loop for a created ferrimagnetic phase. Transformation of the obtained difference loops into two distinct curves according to Von Dobeneck (1996) is used to obtain a simpler interpretation of these complicated curves (Fig. 1c). The half-difference of magnetization between the curves 'a' and 'b' as a function of the applied field is related to the acquisition of the remanent magnetization and will be called the 'remanent' curve for simplicity. The 'induced' curve is, on the other hand, the half-sum of the magnetization in curves 'd' and 'a' as a function of the applied field.

In order to evaluate the significance and interpretive value of the difference hysteresis loops obtained for a collection of rock samples, the initial step in this study is to consider examples of differences of synthetic curves typical for the major ferrimagnetic rock-forming minerals. In Fig. 2, the first row does not show measured curves before and after heating, but hysteresis loops only for the components that are formed or that disappeared during heating. They are only used to calculate difference loops corresponding to well-known appearing or disappearing components. Two such curves are presented when two distinct components are involved. To visualize more easily the shape of the resultant curve (row 2), curves for the disappearing component are presented on row 1 as mirror images (the occurrence of the phase is denoted by a thick line, and the disappearance of the phase by a thin line). The examples shown in Fig. 2 correspond to several combinations of possible alterations.

(i) The mineralogical alteration is simple, representing only the formation (Fig. 2b) or only the disappearance due to transformation (Fig. 2e) of one ferrimagnetic phase. The shape of the loop obtained using eq. (1) is simple and similar to a normal hysteresis loop for a single mineral phase (row 2).

(ii) The alteration corresponds to the occurrence of two ferrimagnetic phases with different coercivities. The loop (row 2) obtained by the difference of the loops measured after successive heating steps is a wasp-waisted or pot-bellied hysteresis loop (Fig. 2, row 2a). In the case of the disappearance of two ferrimagnetic phases with different coercivities, the obtained loop is the mirror image of that shown in Fig. 2(a).

(iii) The alteration corresponds to the formation of one ferrimagnetic phase and the simultaneous disappearance of another ferrimagnetic phase with a different coercivity and saturation field (i.e. mostly the transformation of a magnetic mineral). The difference loop obtained becomes complicated. Figs 2(c) and (d) give the synthetic curves (row 2) obtained in practice by the sum of the two curves from row 1. Rows 3 and 4 in Fig. 2 concern the remanent curve. Row 3 gives these curves for the disappearing and appearing phases separately, and row 4 the sum of these two curves. The central peak on the curve of row 4 corresponds to the phase with the lowest coercive force. If it is oriented towards positive (negative) values, it indicates that the appearing (disappearing) phase has the lowest coercivity. An indication of the coercive force value (Fig. 3) is given by the field associated with the inflection points of the curve. On a simple loop, however, the inflection points do not correspond perfectly to the coercive force, but they are close to this field value. Moreover, summing two curves can introduce a disturbance in the resultant curve, and the inflection points on the latter can be considered only as approximations. Rows 5 and 6 (Fig. 2) show the induced curve. Row 5 gives these curves for the disappearing and appearing phases separately, and row 6 the resultant of these two curves. For the latter, the saturation for the high field with an increase (decrease) of the magnetization is associated with the appearing (disappearing) phase. The peak on the curve for the lower field gives the order of magnitude (Fig. 3) of the beginning of the magnetization saturation (change of curvature of the loop) for the other component.

Fig. 4 presents the same modelling if one of the appearing or disappearing mineral phases is superparamagnetic (i.e. $H_c = 0$). The curve for the remanent part of the loop (row 4) is obviously similar to that (row 3) of the magnetic phase with significant coercivity if a component with zero coercivity is added or subtracted. This is not the case for the curve for the induced part of the loop (rows 5 and 6). Similar cases, but for one of the loops corresponding to the ferrimagnetic phase with coercivity and the other with (Figs 2a and d) or without (Figs 4a and b) coercivity, can be distinguished by the curve for the remanent part (rows 3 and 4), even for wasp-waisted loop.

4 INTERPRETATION METHOD OF THE MEASURED DIFFERENCE OF HYSTERESIS LOOPS

To take into account all the mineralogical alterations occurring during heating, loops have been measured for relatively large samples ($\approx$1 cm^3), thus ensuring that all rock components are included. In the case of magnetic extracts, only the alteration of the pre-existing ferrimagnetic phases should contribute to the observed changes in hysteresis properties.
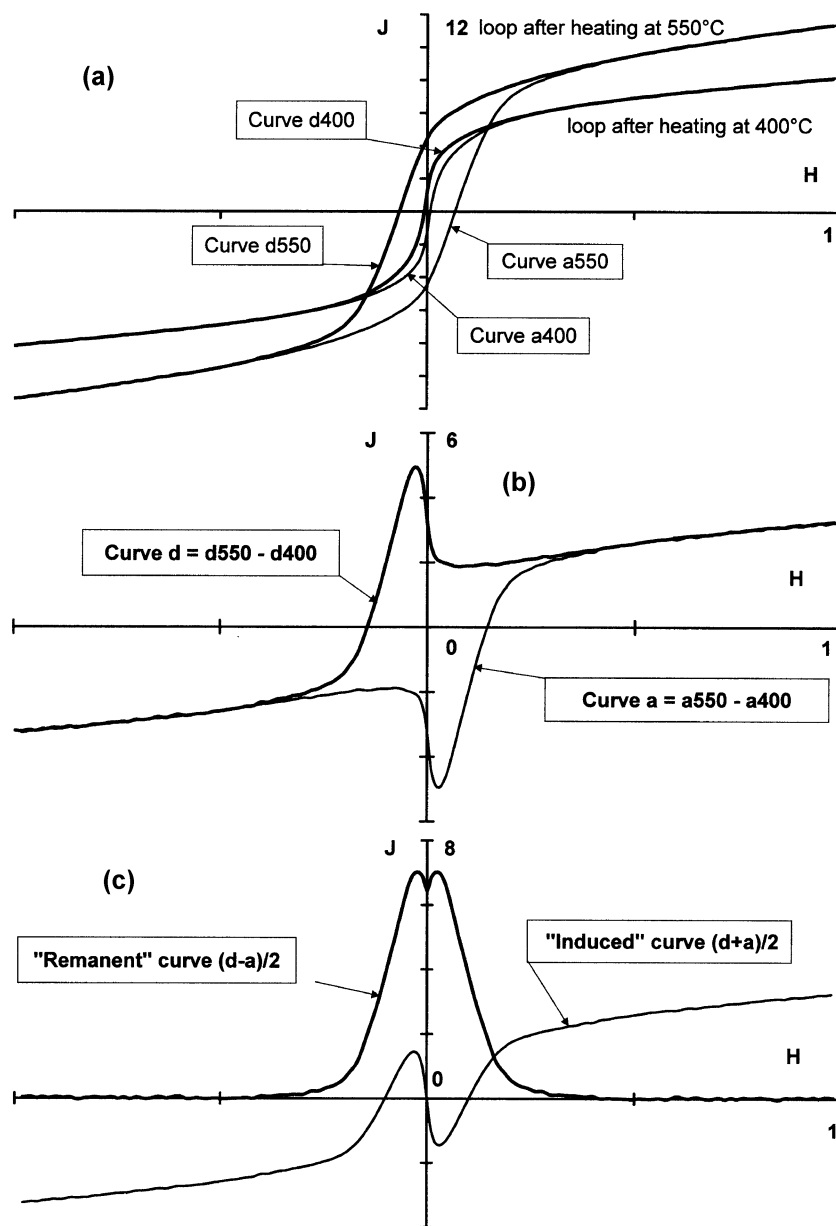
Figure 1. (a) Measured hysteresis loops after heating at 400° and 550°C in dolerite sample D153: 'ascending' (a400 and a550) and 'descending' (d400 and d550) parts of the loops. (b) 'Ascending' (a) and 'descending' (d) parts of the difference loop. (c) Transformation in 'remanent' and 'induced' curves.

The loops were measured in the Saint-Maur laboratory (IPGP) using a laboratory-made translation inductometer within an electromagnet with a maximum applied field of 1 T. The measurements were made at ambient temperature after corresponding heating of the samples in a laboratory-made non-magnetic furnace in air. The value of the magnetic field H corresponding to each measured magnetic moment J is not exactly the same during the measurements of the different loops that have to be subtracted. Thus, smoothing of the curves was applied to determine J values for a given field value. The difference hysteresis loop (eq. 1) is $J_{Tj-Ti}(H)$. $J_{Ti}(H)$ and $J_{Tj}(H)$ are the smoothed curves for temperature steps Ti and Tj (Tj > Ti). To determine variations during progressive heating, difference loops have been calculated for different heating steps T1 < T2 < T3... after the measurement at room temperature T0: curves $J_{T1-T0}(H)$, $J_{T2-T1}(H)$, $J_{T3-T2}(H)$, ... On the curves with very weak difference values, a parasitic effect (periodic signal) related

to the measurement instrument can appear. Depending on the accordance of the periodic signal in the curves $J_{Ti}(H)$ and $J_{Tj}(H)$, the amplitude of the parasitic signal is more or less important in the curve $J_{Tj-Ti}(H)$.

Fig. 5 presents the detailed results (remanent and induced curves) obtained for two samples. The curves appear to be affected to a greater or lesser extent by background noise, particularly for the remanent curve. In the case of strong background noise, the shape of this curve generally yields a rough estimate of the coercivity for the appearing and/or disappearing magnetic phases. For example, for the D94 sample, it is clear that a component with very low coercivity disappeared between 200° and 280°C, but also that another component with slightly higher coercivity appeared after the heating at 320°C. Finally we can sometimes observe similar evolution during following different thermal steps (for DN1 sample, from 320° to 600°C treatments). In this case, the curves can be merged
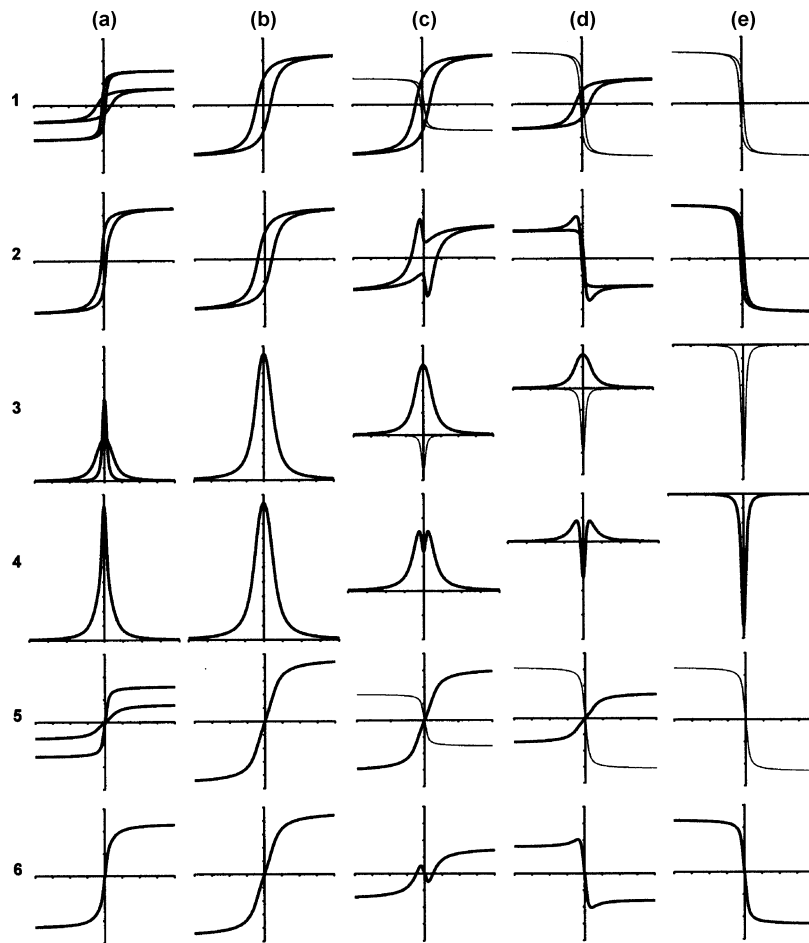
Figure 2. Synthetic hysteresis loops and difference loops for modelling thermal changes occurring during heating. The difference loops shown in row 2 are constructed by summing the appearing (thick line) and disappearing (thin line) components depicted separately in row 1: cases for the appearance of two magnetic phases (a), of appearance of one magnetic phase (b, c and d) together with the disappearance of one magnetic phase (c, d and e). Simple and difference loops are resolved into remanent (rows 3 and 4 respectively) and induced (rows 5 and 6 respectively) curves (see text).
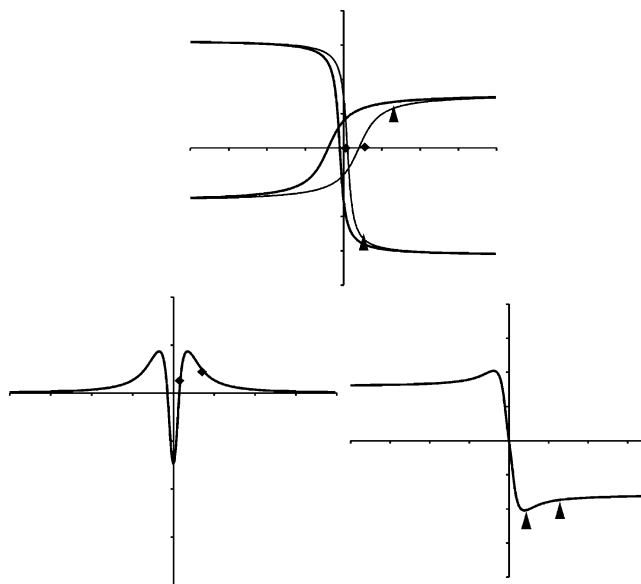
Figure 3. Schematic representation of the estimation of coercive force (diamonds) of appearing and disappearing components on the remanence curve (bottom left graph) and the field strengths at which saturation of magnetization starts (triangles) determined from the induced curve (bottom right graph).

(for example, for DN1, the interpreted curve can be for the 320°–600°C interval). Moreover, we can study in this case the evolution of the mineralogical alteration by comparing the magnetization intensity variation for a given field value during the various steps of the treatment (Fig. 5).

Fig. 5 shows various kinds of differences of hysteresis loops. The following typical examples are indicated in order of ascending complexity.

(i) DN1 600°–320°C evolution is mainly characterized by the disappearance of a component of medium coercivity of about 0.1 T (remanent curve) with a saturation field close to 0.2 T (induced curve). This probably corresponds to the transformation of ferrimagnetics to paramagnetics (or superparamagnetics of lower susceptibility). The regular variation of the saturation magnetization during the various heating steps indicates that this transformation is progressive with temperature, maybe revealing progressive alteration of the same magnetic grains. The small variation of the remanent curve around the very low field perhaps corresponds to a minor alteration of grains of very low coercivity.

(ii) In contrast, the DN1 700°–600°C interval shows the opposite evolution of the remanent part (the occurrence of a component with a coercivity of about 0.05 T) and induced part (the disappearance of a component with a saturation field of about 0.2 T). This probably
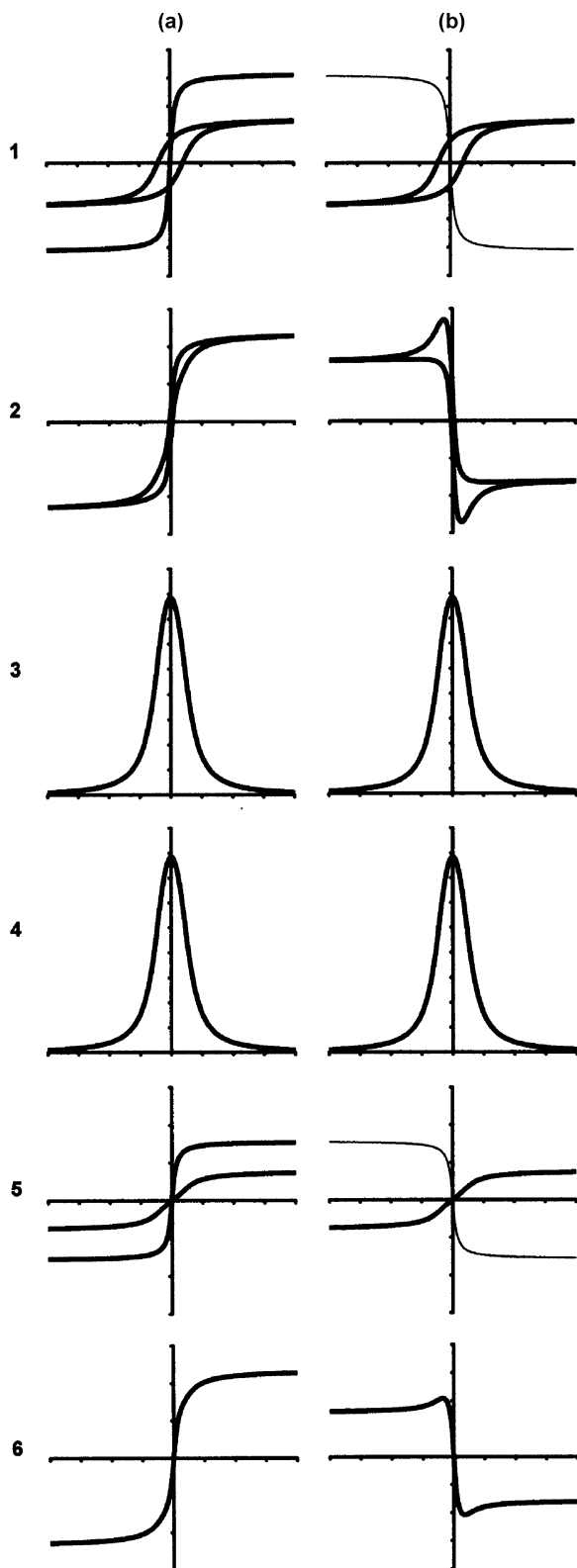
Figure 4. Initial curves (row 1) and modelled difference hysteresis loops (row 2) in the special case when a superparamagnetic component ($H_c = 0$) is present. Remanence parts are shown in row 3 (individual curves for each component) and row 4 (curve for the difference loop). Induced parts are shown in row 5 (individual curves for each component) and row 6 (curve for the difference loop).

indicates transformation of a ferrimagnetic phase, maybe related to grain-size variation. Such a case will be called 'transformation' in this paper.

(iii) The D94 400°–320°C example is already more complicated. Except for very low fields, the induced curve corresponds to the formation of a component with a high saturation field (no full saturation at 1 T). The remanent curve shows the occurrence of a component of coercivity of about 0.05 T. These curves could indicate the formation of the same component. However, for very low field values, the induced curve indicates the disappearance of a component of very low coercivity or of one that is superparamagnetic.

(iv) The DN1 120°–20°C curves show at the same time two opposite evolutions: the disappearance of a component of high (about 0.15 T) coercivity and a high saturation field (no full saturation) and the occurrence of a magnetic phase with lower (about 0.04 T) coercivity and a saturation field (about 0.1 T). We can notice that DN1 200°–120°C shows very similar mineralogical alteration, except that the remanent curve does not indicate the formation of a low-coercivity component, probably showing that the new component formed is superparamagnetic.

(v) The D94 700°–600°C induced curve appears to be more complicated. It is, however, clear that we have the occurrence of a component with a high saturation field (no full saturation) and the disappearance of a medium saturation field phase (about 0.2 T), but the interpretation of the very small variation for the very low field is not so clear. Probably, it reflects the occurrence of a component with a very low saturation field, having on the resultant curve an almost opposite effect to the disappearance of the medium saturation field component. The remanent curve is simpler, showing only the disappearance of the medium-coercivity (about 0.1 T) component and the small occurrence of a small amount of a very low-coercivity component.

5 EXAMPLES

Estimates of the coercive force and of the magnetization saturation for the appearing and/or disappearing magnetic phase(s) for various samples are presented in Fig. 6. Examples of practical applications of the estimates shown are grouped below according to their magnetic mineralogy, revealed by thermomagnetic $K(T)$ analysis (KLY3 Kappabridge, Agico, Brno) combined with SEM/EDX data for some of the samples. Thus, the potential of the new approach of using difference hysteresis loops to constrain better the mineralogical alterations appearing during laboratory heating is presented for typical rock-forming mineralogies of intrusive rocks (diorites and gabbro-diorites from Hesperides pluton and dykes from Livingston island, Antarctica, and Ti-rich Devonian dolerites from southern Algeria), basalts (Crozet island), ankeritic shelly clays and redbeds (eastern and southern Algeria), and Pliocene volcanoclastic sandstones (Eastern Rhodopes, Bulgaria).

5.1 Intrusive rocks: pluton (H03) and dykes (DN1 and KD2A) from Livingston island, Antarctica

The examples from intrusive rocks (Henry *et al.* 2003; Jordanova *et al.* 2005) possess typical behaviour of thermomagnetic curves (susceptibility in low field as a function of temperature—$K(T)$ curve), showing a slight but well-expressed increase of susceptibility at 120°–130°C during heating, followed by a significant decrease in the signal at about 320°–350°C. The final steep decrease at 590°C indicates a magnetite Curie point (Figs 7b and d). Partial $K(T)$ runs show that the changes up to 350°C are irreversible. The
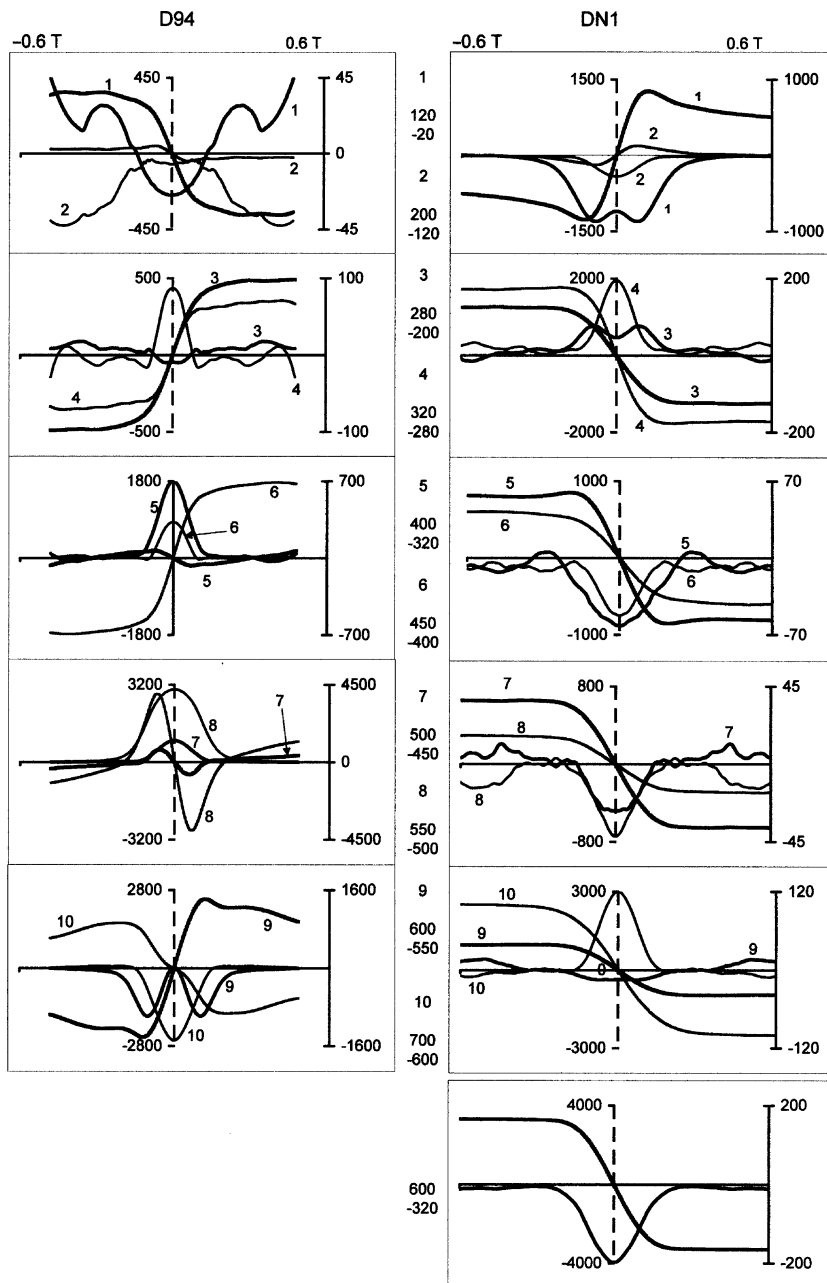
Figure 5. Difference loops for two of the studied samples: curves for the remanent and induced parts. Field in T and magnetization in mA m^2 kg^{-1}, scale in the middle and on the right for the induced and remanent curves respectively.

cooling curve suggests the presence of a small quantity of haematite and magnetite. The chemical composition of dykes deduced from EMPA (sample DN1—Fig. 7a) and diorites from SEM/EDX analysis (sample H03—Fig. 7c) points to a titanomagnetite with varying Ti-content. The latter is more significant in the diorite sample H03, while in dyke DN1 (microporphyritic diorite) the calculated composition on the base of four oxygen ions is Fe$_{3-x}$Ti$_x$O$_4$, with $x = 0.134$. The presence of some degree of low-temperature oxidation (maghemitization of the initial titanomagnetite) may be inferred from the observed brighter regions in the grains. The SEM picture for the sample from Hesperides pluton (H03) reveals the presence of granulation, which is probably a result of secondary hydrothermal alteration of granites, that is widely found in the rocks of the pluton and the dykes cutting it (Zheng *et al.* 2003). The observed granula-

tion texture was identified as a product of hydrothermal alteration in the study of basalts by Ade-Hall *et al.* (1971).

From the above-mentioned data on the magnetic carriers and the phase composition of the samples, further information on the thermal stability and evolution of ferrimagnetic carriers is obtained by the analysis of the induced and remanent parts of the difference hysteresis curves. Fig. 5 shows the resulting curves for the dyke sample DN1. The variations of the absolute values of the classical hysteresis parameters determined in the various measured loops, namely coercive force H_c, coercivity of remanence H_{cr}, saturation magnetization J_s, and saturation remanence J_{rs}, are given in addition (Fig. 8) for clarity. It is obvious that the relatively high coercivity exhibited by the sample is due to the phase that is destroyed at relatively low temperature. The exact processes/alterations that take place during
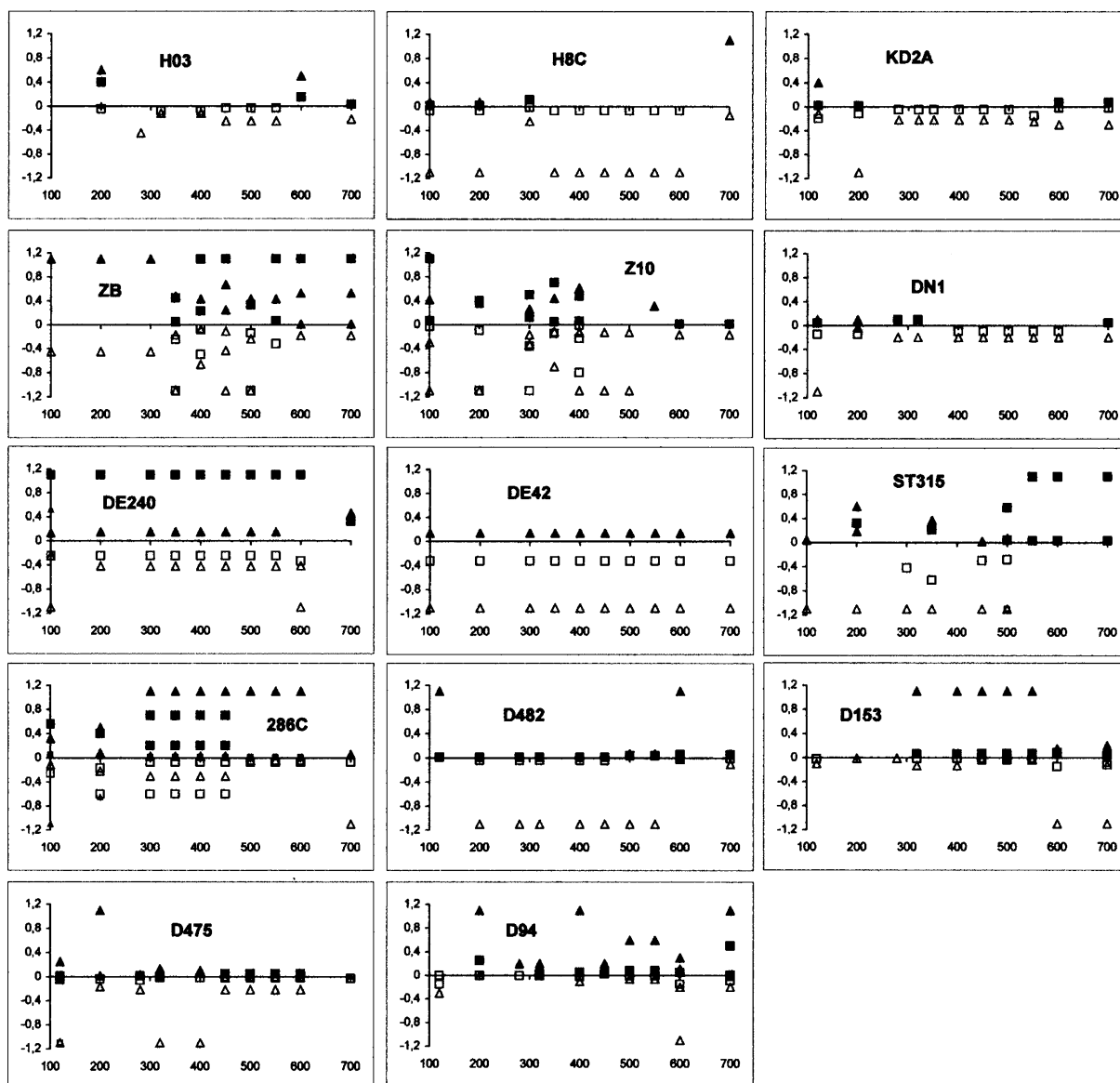
Figure 6. Estimates of coercive forces (squares) and field strengths necessary for saturation of magnetization components (triangles) for appearing (open symbols) and disappearing (full symbols) magnetic phases as a function of temperature. Field in T.

heating can be well followed by the difference hysteresis loops and the corresponding remanent parts, used as a proxy for the coercivity of the new/disappeared phases during heating. As a result of heating to 120°C, difference loops show the destruction of a high-coercivity phase accompanied by the formation of a new low-coercivity phase with higher saturation magnetization. This evolution is continued with heating up to 200°C, but with significantly weaker intensity and without the formation of a low-coercivity phase. Let us consider the observed features on the heating $K(T)$ curve (Fig. 7b), results from microprobe analysis and SEM observations in the context of the obtained difference loops (Fig. 5). As a result of the initial heating to 120°C, a new strongly magnetic phase with moderate coercivity appears. At the same time, the high-coercivity phase, which does not reach saturation in a 0.6-T field, is destroyed. The next heating step (200°–120°C) causes the disappearance of a further high-coercivity phase, but now at the same time there appears a strongly magnetic phase, which is not seen on the remanence curve. Starting at the 280°C step (subtraction plot 280°–200°C), the in-

ducted curve indicates the disappearance of a strongly magnetic phase with a coercivity of about 0.2 T. As a result of heating to 320°C (320°–280°C curves in Fig. 8a), the intense destruction of a strongly magnetic and soft superparamagnetic (SP) component is accompanied by the creation of a magnetically hard phase with low magnetization. Thermal steps up to this temperature correspond to the particular $K(T)$ behaviour (Fig. 7b). The described evolution can be linked to the process of temperature-induced inversion of low-Ti titanomagnetite/titanomaghemite in the following way. The process starts with stress release after heating to 120°C, causing the observed appearance of a phase with lower coercivity. On the next heating step, this new phase probably becomes SP due to further lab-induced oxidation. After 280°C, we still have some of the initial titanomaghemite grains preserved, which give the observed disappearing component on the remanence curves. Further stages in the process of titanomaghemite inversion are probably achieved after heating to 320°C, where difference curves indicate the disappearance of a weakly magnetic component with moderate coercivity.
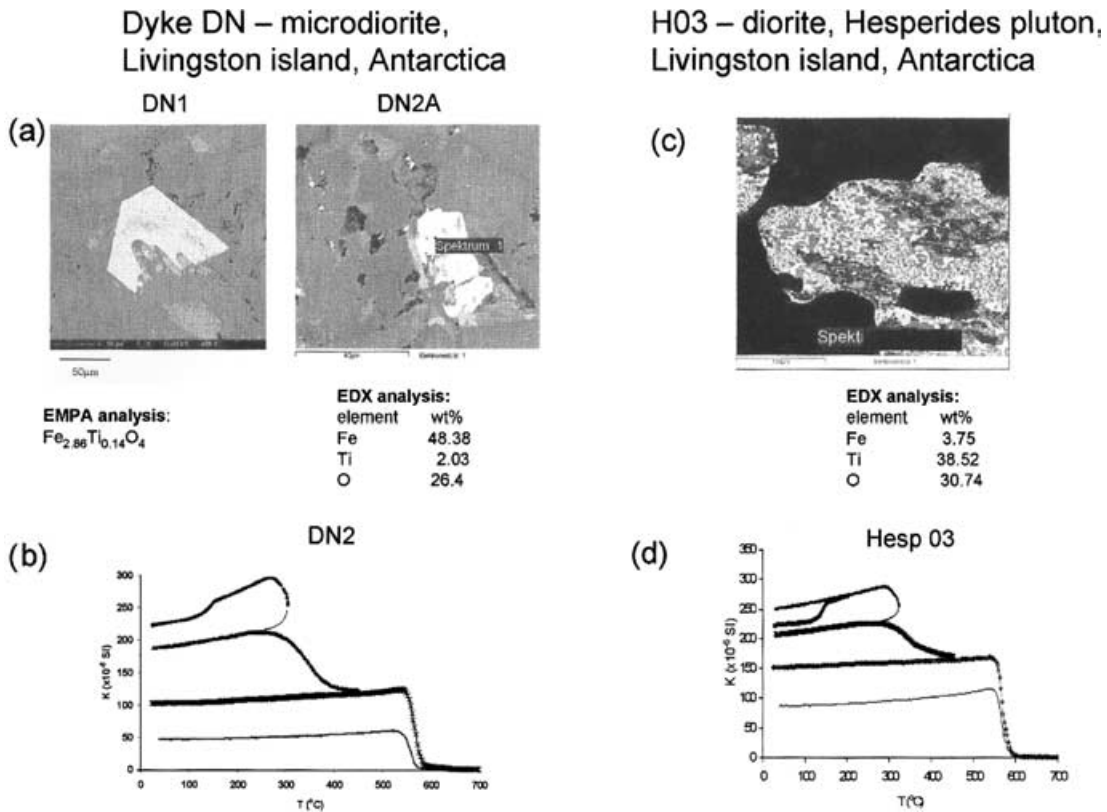
Figure 7. Magnetic mineralogy of samples DN and H03 from the intrusive rocks (Livingston island, Antarctica) deduced from SEM pictures, electron microprobe analysis (EMPA), EDX analysis (a: samples DN; c: sample H03) and thermomagnetic analysis of magnetic susceptibility $K(T)$ in samples DN2(b) and H03 (d), with partial runs (done in air).
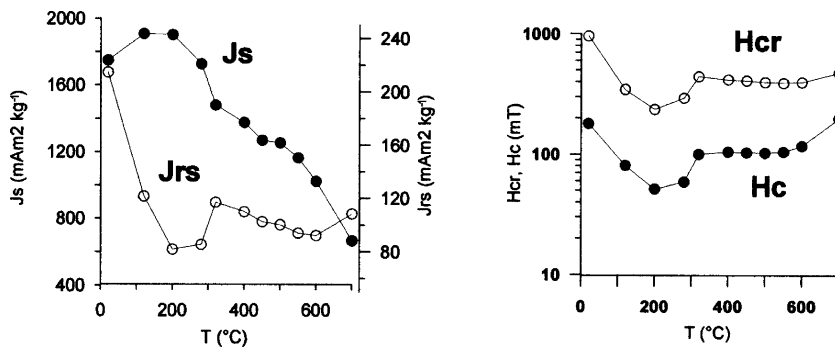

Figure 8. Variations of the absolute values of the hysteresis parameters (J_s, J_{rs}, H_c, H_{cr}) measured after successive heating steps for sample DN1.

Further heating (combined steps from 320° to 600°C which show similar behaviour) causes the simple process of the disappearance of a strongly magnetic phase, probably caused by progressive oxidation of the created spinel phase due to inversion after 320°C. After 700°C some haematite is obviously created.

The variations of the absolute values of hysteresis parameters (Fig. 8b) fit well with the described mineralogical/phase transformations.

A similar evolution of the difference hysteresis loops is observed for another sample from a dyke (sample KD2A). Exactly the same as for the first dyke DN, thermal $K(T)$ behaviour (Fig. 9b) is accompanied by the disappearance of a high-coercivity component after 120°C and a less well-expressed formation of a new soft phase (different scales for J_s and J_{rs}). The main process of the disappearance of the soft component prevailed already at 200°C. Taking into

account the significantly lower H_{cr} values for this sample in comparison with DN1, we can suppose a smaller effective grain size of titanomaghemites. Thus, the process of stress release and inversion is moved to lower temperatures. This is probably the reason that the remanence curves up to 320°C have very low intensities (note the scale) and their interpretation is not easy. For the same reason, the progressive behaviour after the 400°–320°C step is not so coherent, and the transformation to rhombohedral haematite starts after the 600°C heating step and is more pronounced (Figs 9a and c).

The diorite sample H03, which clearly shows an overall granulation texture in the titanomagnetite grains (Fig. 7c) exhibits magnetically soft behaviour due to the large grain size. However, the difference curves (Fig. 10a) indicate the three temperature intervals with the most significant processes of oxidation of magnetization carriers—300° to 600°C.
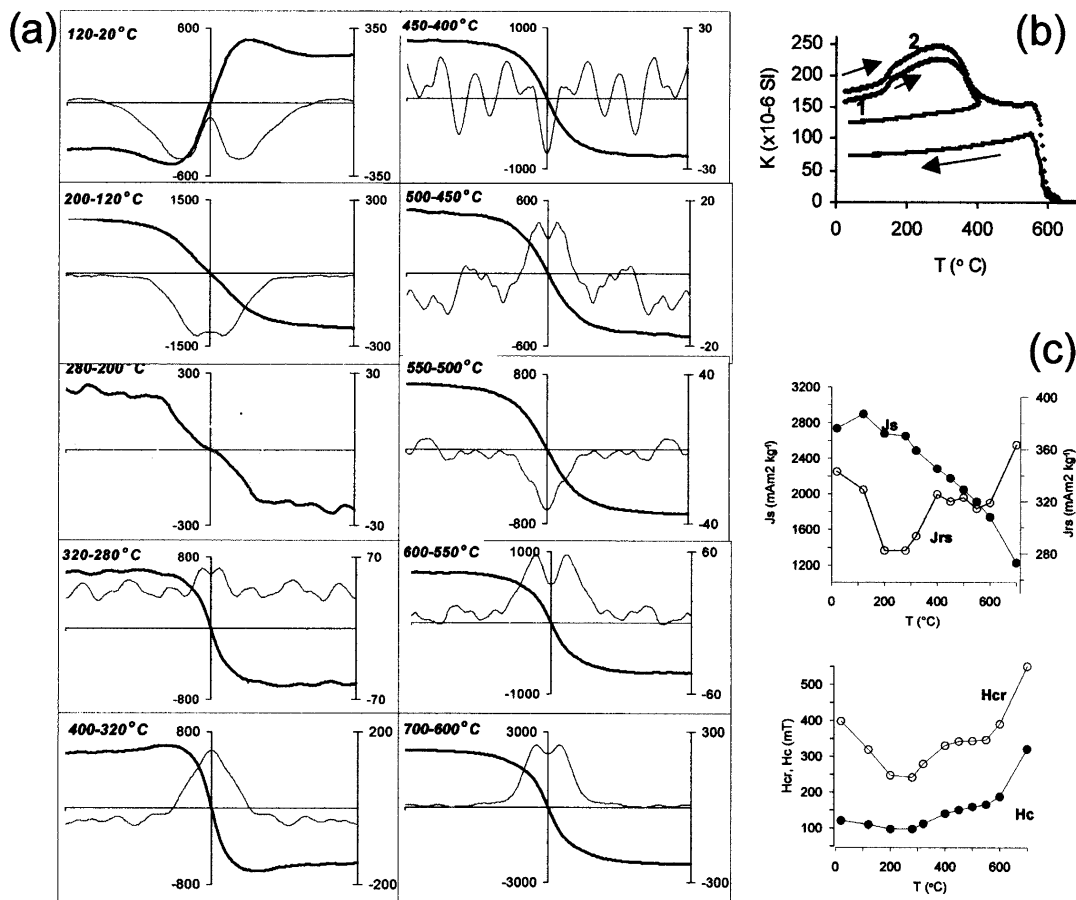
Figure 9. Results for sample KD2A. (a) Difference loops (induced curve in grey, remanent in black; field is from −0.5 to 0.5 T and magnetization in mA m^2 kg^{-1}, scale in the middle and on the right for induced and remanent curves respectively); (b) thermomagnetic $K(T)$ analysis in air for two samples (indicated 1 and 2); and (c) variations of the absolute values of the hysteresis parameters (J_s, J_{rs}, H_c, H_{cr}) measured after successive heating steps.
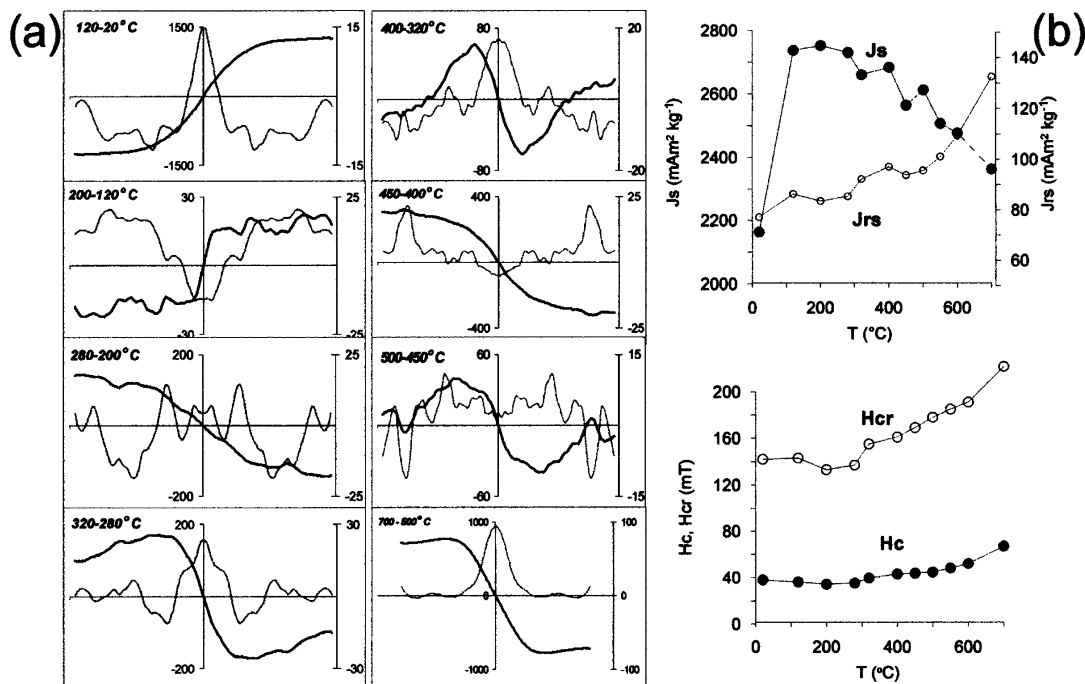

Figure 10. Results for sample H03. (a) Difference loops (induced curve in grey, remanent in black; field is from −0.5 to 0.5 T and magnetization in mA m^2 kg^{-1}, scale in the middle and on the right for induced and remanent curves respectively); (b) variations of the absolute values of the hysteresis parameters (J_s, J_{rs}, H_c, H_{cr}) measured after successive heating steps.
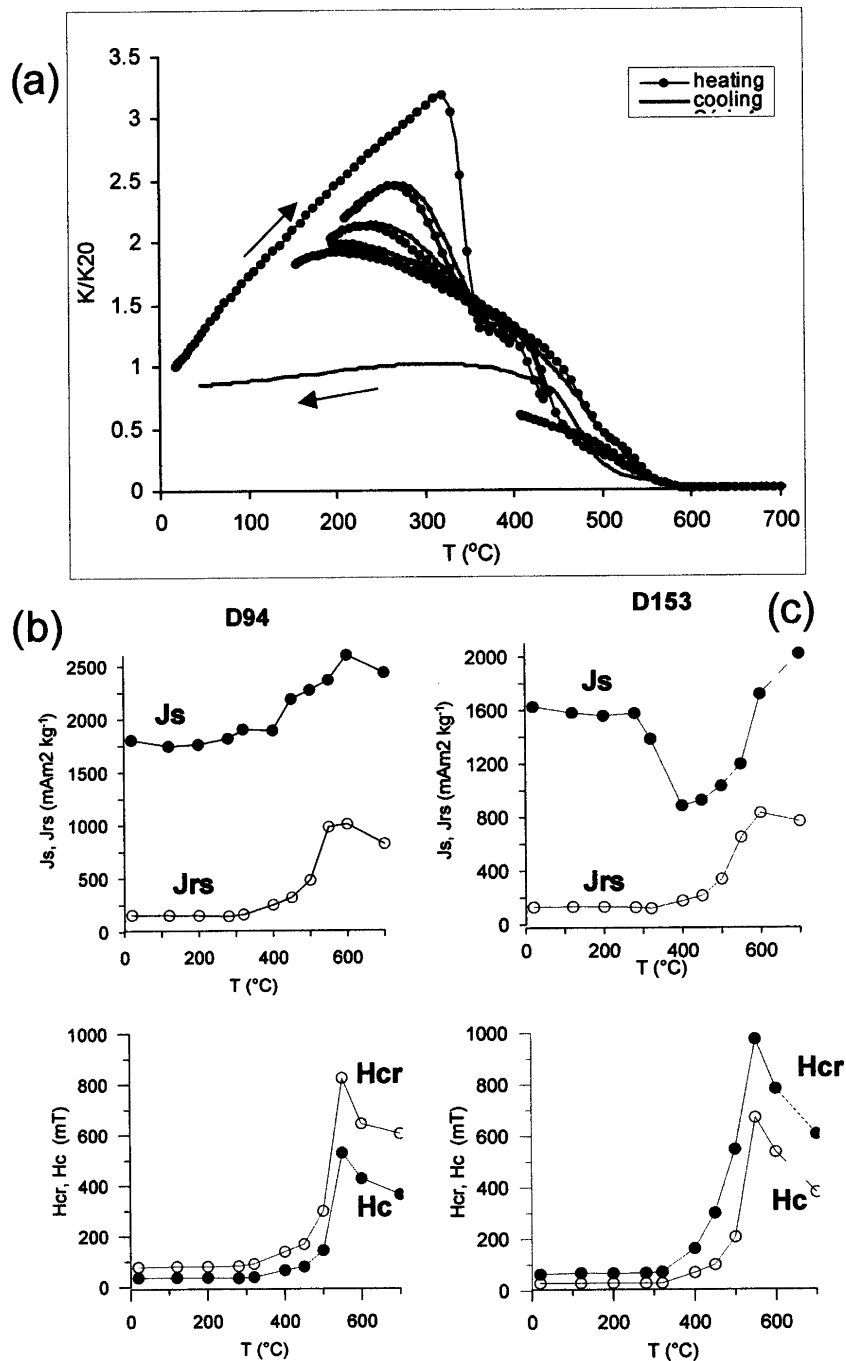
Figure 11. Thermomagnetic $K(T)$ analysis for the dolerite sample D94 (a), and variations of the absolute values of the hysteresis parameters (J_s, J_{rs}, H_c, H_{cr}) measured after successive heating steps for samples D94 (b) and D153 (c).

5.2 Ti-rich dolerites (D94 and D153) from southern Algeria

The behaviour of magnetic susceptibility during heating–cooling cycles for the dolerite sample D94 (Fig. 11a) reveals a continuous thermal evolution of mineralogy from heating above 350°C (Derder *et al.* 2005; Jordanova *et al.* 2005). Partial runs to lower temperatures, carried out at different steps, show a systematic lowering of the maximum enhancement, and the position of this enhancement on the temperature scale moves towards lower values. Consequently, there is an irreversible change in microstructure, insofar as

the values of the hysteresis parameters measured after subsequent heating steps (Fig. 11b) do not change significantly up to 300°C. The strong initial increase of susceptibility during thermomagnetic analysis and the subsequent changes described above probably result from the unblocking of small titanomagnetite grains and an effective superparamagnetic state at 300°C. Grain growth during heating and subsequent partial $K(T)$ runs leads to a systematic decrease in the maximum K-values as well as the lowering of the temperature at Kmax. After 300°C, major mineralogical changes occur, as is seen by the significant increase in magnetization values (both J_s and J_{rs}), accompanied by an increase in hardness (Fig. 11b) up to
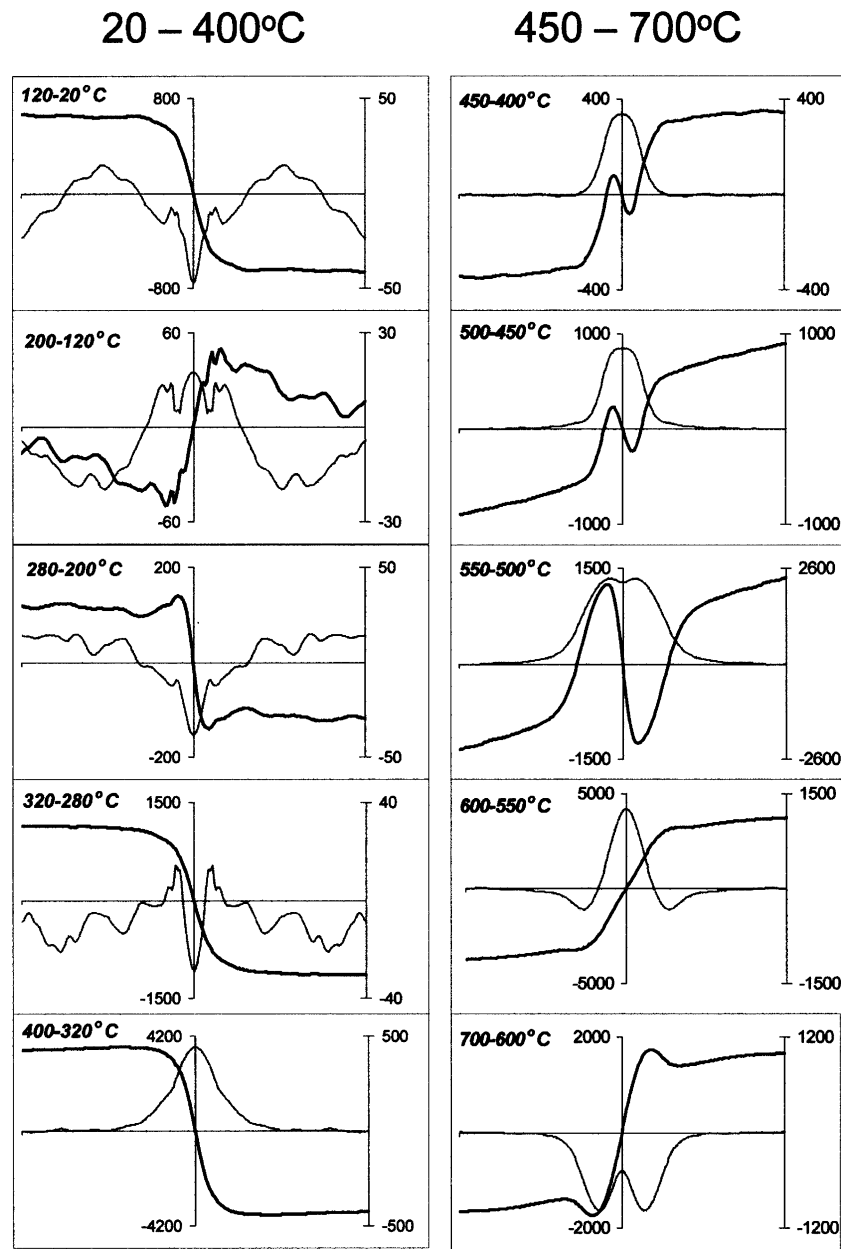
20 – 400°C   450 – 700°C

Figure 12. Difference loops (induced curve in grey, remanent in black) obtained for the dolerite sample D153 (field is from -0.5 to 0.5 T, magnetization in mA m^2 kg^{-1}, scale in the middle and on the right for induced and remanent curves respectively).
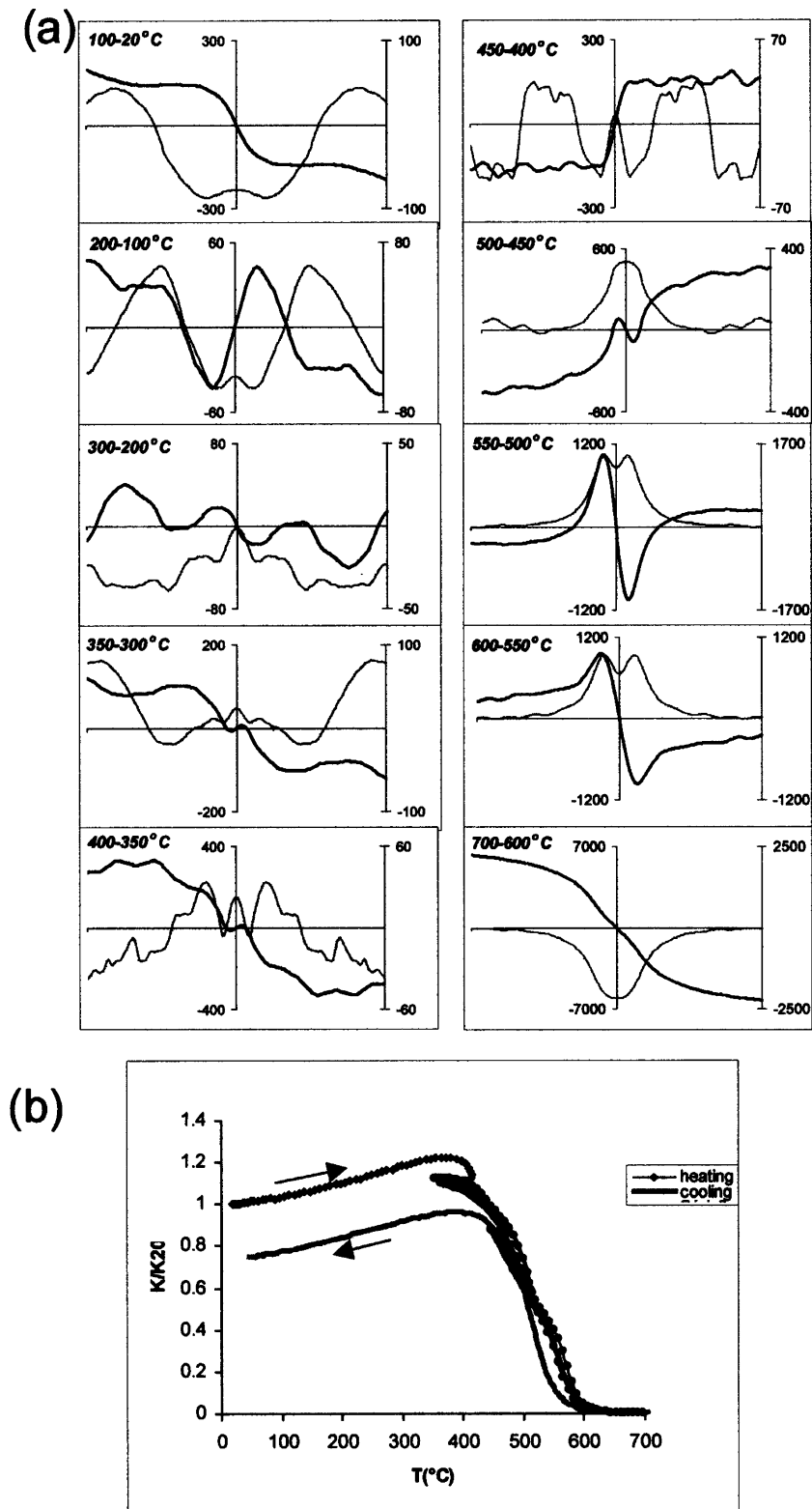
500°C. These changes can be better resolved by difference hysteresis curves (Fig. 5). High-temperature deuteric oxidation (inversion) of Ti-rich titanomaghemite resulting in the formation of a Ti-poor titanomagnetite phase is probably the alteration behind the changes. The destruction of the latter at higher temperatures (550°–600°C and 600°–700°C) and the formation of a new soft phase is reflected in the remanence curves (Fig. 5).

A second dolerite sample from the same locality (D153) shows similar behaviour, with the difference expressed by the presence of a significantly better presented magnetically soft component, which is destroyed at low temperatures up to 320°–400°C (Fig. 12). High-temperature oxidation, starting at the 400°C heating step, is very well resolved by the obtained difference loops. Starting with the interval 450°–400°C, the process is expressed by the creation of a more strongly magnetic Ti-poor spinel phase (magnetite?) with

medium coercivity and, at the same time, the disappearance of a SP phase. The relative proportion of the latter increases steadily from the 400°C to 500°C step. It is probably connected with the speed of high-temperature oxyexsolution and growth of the magnetite-like phase. The continued process after 550°C leads to the observed lowering of coercivity parameters (Fig. 11c). This is expressed on the difference curves by the disappearance of a hard component and the appearance of a soft one (Fig. 12, steps 600°–550°C and 700°–600°C).

5.3 Basalts (286C) from Crozet Island

The partial oxidation of magnetite to haematite during thermal treatment is manifested in the thermomagnetic analysis (Fig. 13b) of a basalt sample from Crozet Island (Camps *et al.* 2001). Clear

Figure 13. (a) Difference loops (induced curve in grey, remanent in black) obtained for the basalt sample 286c (field is from -0.5 to 0.5 T and magnetization in mA m^2 kg^{-1}, scale in the middle and on the right for induced and remanent curves respectively). (b) Thermomagnetic $K(T)$ analysis (in air).

evidence concerning the nature of this alteration lies in the behaviour of the difference loops (Fig. 13a). Changes in magnetic mineralogy up to temperatures of 450°C are obscured by the weak difference signal. An additional complication is the presence of out-of-phase noise harmonics for the two subtraction curves. Thus, the

interpretive information can be gained from the temperature steps after 450°C (Fig. 13a), where the difference curves (both induced and remanent) have higher intensity. They clearly show, as a result of 500°–550°C and 550°–600°C heatings, the disappearance of a soft magnetic phase and the formation of a harder one. This
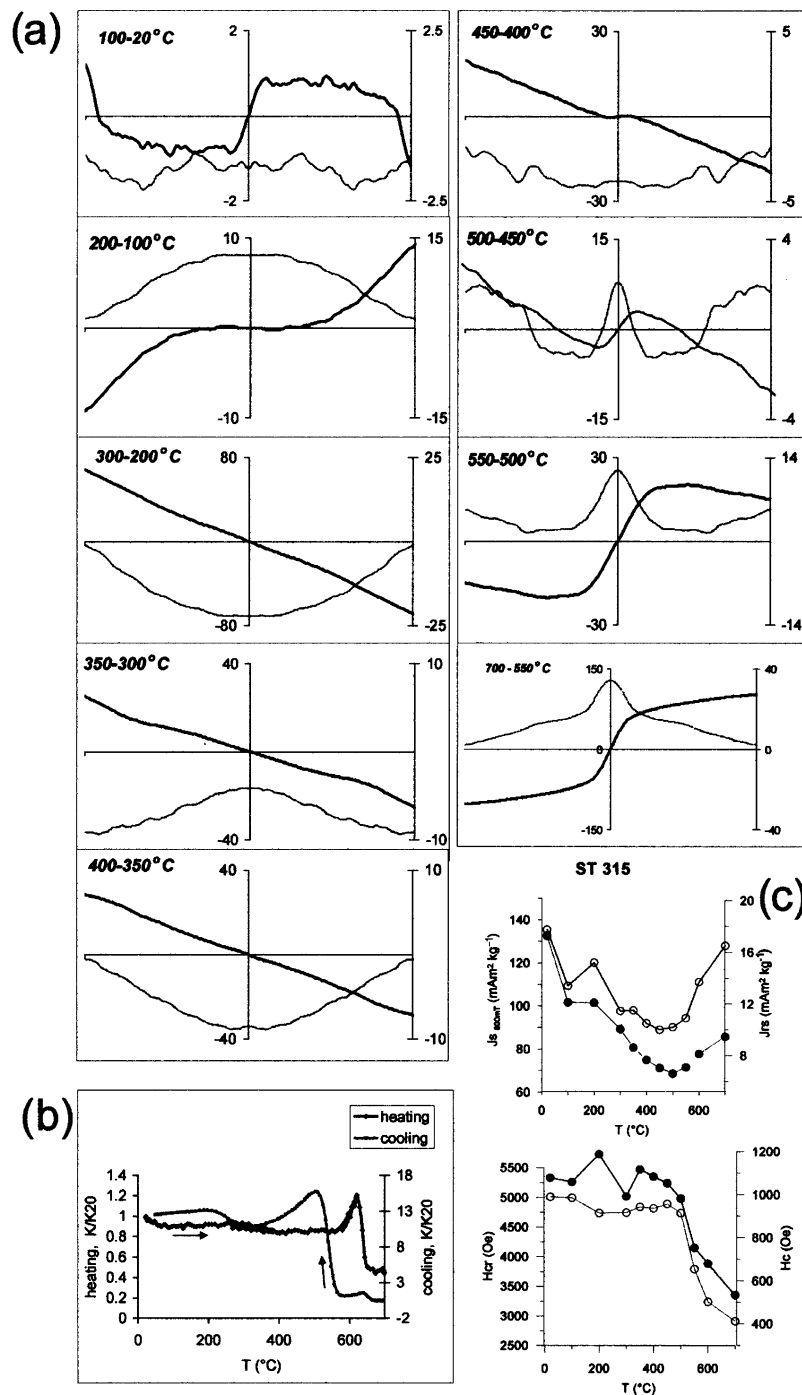
Figure 14. Results obtained for a haematite-bearing ankeritic limestone (sample ST315). (a) Difference loops (induced curve in grey, remanent in black; field is in T and magnetization in mA m^2 kg^{-1}, scale in the middle and on the right for induced and remanent curves respectively); (b) thermomagnetic $K(T)$ analysis (in air); and (c) variations of the absolute values of the hysteresis parameters (J_s, J_{rs}, H_c, H_{cr}) measured after successive heating steps.

behaviour probably corresponds to the progressive oxidation towards haematite. The final destruction of the formed hard component is reached after heating at 700°C, suggesting that the haematite phase probably reaches a larger effective grain size.

5.4 Ankeritic shelly limestone (ST315) and redbeds (DE42 and DE 240) from eastern and southern Algeria

Typical examples for haematite-bearing sediments are the studied ankeritic limestones from eastern Algeria (Henry *et al.* 2004).

Thermomagnetic analysis of magnetic susceptibility indicates that haematite is the major ferromagnetic carrier, as evidenced by the well-expressed Hopkinson peak before the steep decrease of the signal at 670°C on the heating curve (Fig. 14b). An initial small decrease up to 100°C is also evident. The creation of a new strongly magnetic phase with a Curie temperature (Tc) of 580°C occurs during the cooling cycle.

A precise picture of the observed alterations is given by the difference loops in Fig. 14(a). The initial formation of a phase with extremely high coercivity probably indicates goethite dehydration

and the formation of haematite. A further increase of the mean grain size of this newly formed haematite is probably the reason for the disappearance of the hard phase after heating at 300°, 350° and 400°C, with growth of the crystals passing the pseudo-single-domain/multidomain (PSD/MD) threshold for haematite (Dunlop & Özdemir 1997). Thermally induced mineralogical changes in the ankeritic clay minerals at higher temperatures result in the observed formation of a soft magnetic phase in the interval 450°–550°C (Fig. 14a). Continuous oxidation towards haematite and the formation of new magnetite is probably the reason for the wasp-wasted difference hysteresis loop and the corresponding particular shape of the induced and remanent curves for the interval 550°–700°C.

The formation of magnetite due to the destruction of ankerite is also indicated by the absolute values of the magnetization parameters J_s and J_{rs}, which show a significant increase after 500°C (Fig. 14c).

Redbeds (samples DE42 and DE240) from the same area (Henry et al. 2004) show almost perfectly reversible $K(T)$ curves with a well-expressed Hopkinson indicating haematite as the major ferromagnetic carrier. Only a weak decrease of susceptibility at about 300°C corresponds to an irreversible transformation in the sample DE42. However, difference of hysteresis loops clearly point out thermal changes in these rocks. These changes are weak and very similar, but appear at every thermal treatment after low-temperature heating (Fig. 6).
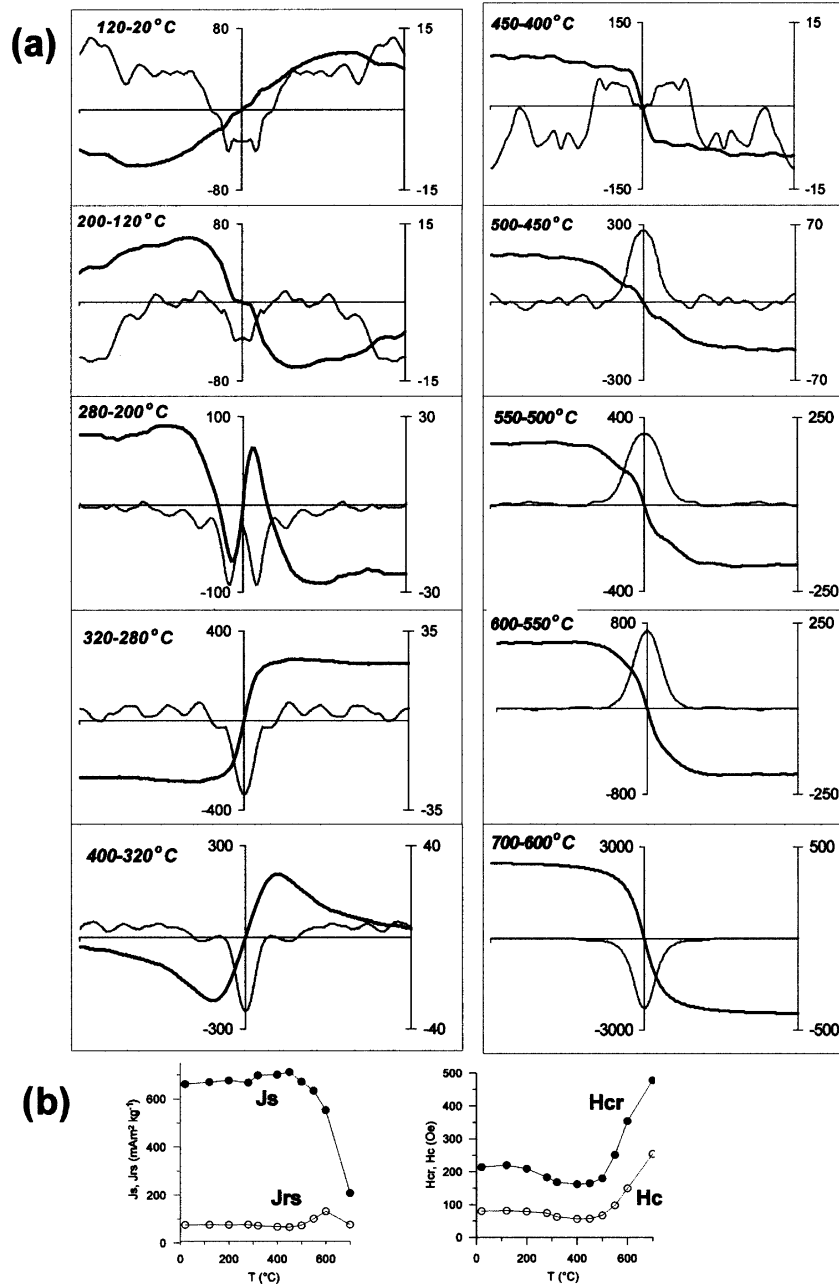

Figure 15. Results obtained for volcanoclastic sandstone (sample D475). (a) Difference loops (induced curve in grey, remanent in black). Field is in T, magnetization in mA m^2 kg^{-1}, scale in the middle and on the right for induced and remanent curves respectively. (b) Variations of the absolute values of the hysteresis parameters (J_s, J_{rs}, H_c, H_{cr}) measured after successive heating steps.

5.5 Pliocene volcanoclastic sandstones (D475) from eastern Rhodopes, Bulgaria

Titanomagnetite carriers in volcanoclastic sediments (Karloukovski 2000) show a distinct behaviour of the induced and remanent parts of the difference hysteresis curves (Fig. 15). The variations of the absolute values of hysteresis parameters indicate relative thermal stability of the rock constituents, including the original ferrimagnetic fraction. Significant changes occur after 450°C. However, closer inspection of the behaviour of the difference loops (Fig. 15) suggests that up to 450°C there is the formation of a new soft magnetic fraction in relatively small amounts (taking into account the magnetization values of the difference loops) and the disappearance of a component with higher coercivity. At temperatures higher than 450°C, this soft phase together with the unchanged original magnetic carrier are transformed into a harder one, deduced from the characteristic shape and position of the difference curves for $T >$ 450°C. The final oxidation of the initial titanomagnetite is reached at temperatures up to 700°C, which is well expressed by the disappearance of a soft component with the highest magnetization after the final heating step (Fig. 15a).

The thermal changes (although relatively small) identified through difference hysteresis loops explain the reason why the characteristic ChRM direction of NRM has been obtained only from AF demagnetization (Karloukovski 2000).

6 CONCLUSIONS

The new approach proposed in this study for tracking mineralogical changes during laboratory heating experiments is a useful tool for better revealing the underlying reasons for the observed variations of the bulk hysteresis parameters with successive heating. Particularly helpful information can be obtained on the processes of grain growth, oxidation, stress release, and finally, phase transformations. The shape of the difference loops and their position relative to the field axis gives a rough estimate on the presence of single phase change or the simultaneous appearance/disappearance of two phases with different coercivities. In the case of a strong enough signal of the difference loops, remanence curves can be used as proxies for the coercivities of the changing phases. Used in conjunction with other diagnostic experiments (rock magnetism, microscopy, etc.), the method gives straightforward information about the nature of the observed behaviour of different rocks. Mineralogical alterations clearly appear already at low-temperature treatment in the studied examples, concerning magmatic as well as sedimentary rocks, containing iron oxides and hydroxides.

REFERENCES

Ade-Hall, J.M., Palmer, H.C. & Hubbard, T.P., 1971. The magnetic and opaque petrological response of basalts to regional hydrothermal alteration, *Geophys. J. R. astr. Soc.,* **24,** 137–174.

Bina, M., Corpel, J., Daly, L. & Debeglia, N., 1991. Transformation de la pyrrhotite en magnetite sous l'effet de la température: une source potentielle d'anomalies magnétiques, *Compt. Rend. Acad. Sci. Paris,* **313**(II), 487–494.

Camps, P., Henry, B., Prévot, M. & Faynot, L., 2001. Geomagnetic palaeosecular variation recorded in Plio-Pleistocene volcanic rocks from the Possession Island (Crozet Archipelago, Southern Indian ocean), *J. geophys. Res.,* **106,** 1961–1972.

Dekkers, M.J., 1990a. Magnetic monitoring of pyrrhotite alteration during thermal demagnetisation, *Geophys. Res. Lett.,* **17,** 779–782.

Dekkers, M.J., 1990b. Magnetic properties of natural goethite—III. Magnetic behaviour and properties of minerals originating from goethite dehydration during thermal demagnetisation, *Geophys. J. Int.,* **103,** 233–250.

Derder, M.E.M. *et al.,* 2005. New African Upper Devonian palaeomagnetic pole from intrusive rocks of the Tin Serririne basin (Southern border of the Hoggar, Algeria), *Geophys. J. Int.,* submitted.

Dunlop, D. & Özdemir, Ö., 1997. *Rock Magnetism,* Fundamentals and Frontiers, Cambridge Univ. Press, Cambridge.

Gehring, A.U. & Heller, F., 1989. Timing of natural remanent magnetization in ferriferous limestones from the Swiss Jura mountains, *Earth planet. Sci. Lett.,* **93,** 261–272.

Henry, B., Jordanova, D., Jordanova, N., Souque, C. & Robion, P., 2003. Anisotropy of magnetic susceptibility of heated rocks, *Tectonophysics,* **366,** 241–258.

Henry, B., Merabet, N., Derder, M.E.M. & Bayou, B., 2004. Chemical remagnetizations in the Illizi basin (Saharan craton, Algeria), *Geophys. J. Int.,* **156,** 200–212.

Hirt, A.M. & Gehring, A.U., 1991. Thermal alteration of the magnetic mineralogy in ferruginous rocks, *J. geophys. Res.,* **96,** 9947–9953.

Jordanova, N., Jordanova, D., Henry, B., Derder, M.E.M., Bayou, B. & Amenna, M., 2005. Ferrimagnetic fabric from AMS of heated rocks, *Geophys. J. Int*, in preparation.

Karloukovski, V., 2000. Magnetostratigraphy and palaeomagnetism of the area around the Momchilgrad Palaeogene depression, the East Rhodope massif, *PhD thesis,* University of East Anglia, Norwich.

Özdemir, Ö., 1990. High temperature hysteresis and thermoremanence of single-domain maghemite, *Phys. Earth planet. Inter.,* **65,** 125–136.

Schwartz, E.J. & Vaughan, D.J., 1972. Magnetic phase relations of pyrrhotite, *J. Geomag. Geoelectr.,* **24,** 441–458.

Van Velzen, A.J. & Zijderveld, J.D.A., 1992. A method to study alterations of magnetic minerals during thermal demagnetization applied to a fine-grained marine marl (Trubi formation, Sicily), *Geophys. J. Int.,* **110,** 79–90.

Verwey, 1935. The crystal structure of γFe_2O_3 and γAl_2O_3, *Z. Krist.,* **91,** 65–69.

Von Dobeneck, T., 1996. A systematic analysis of natural magnetic mineral assemblages based on modeling hysteresis loops with coercivity-related hyperbolic basis functions, *Geophys. J. Int.,* **124,** 675–694.

Zheng, X., Kamenov, B., Sang, P. Momchev, 2003. New radiometric dating of the dykes from the Hurd peninsula, Livingston island, South Shetland Islands, *J. South Am. Earth Sci.,* **15,** 925–934.